Supplement of Hydrol. Earth Syst. Sci., 26, 6413–6426, 2022
https://doi.org/10.5194/hess-26-6413-2022-supplement

Hydrology and Earth System Sciences
Open Access

Supplement of

Spatial distribution of oceanic moisture contributions to precipitation over the Tibetan Plateau

Ying Li et al.

Correspondence to: Ying Li (ly_hyrdo@outlook.com) and Hui Peng (hpeng1976@163.com)

Supplementary

Table S1: Summary of numerical moisture tracking studies over the TP region.

Reference	Study area	Time period	Model	Data	Main conclusions
Chen et al. (2012)	TP	2005–2009 (summer)	FLEXPART	NCEP/GFS	The ocean source could extend from the Arabian Sea to the Southern Hemisphere.
Sun and Wang (2014)	Grassland on eastern TP	2000–2009	FLEXPART	NCEP-CFSR	During the warm (cold) season, oceanic moisture is mainly from the Arabian Sea and Bay of Bengal (areas surrounding the Arabian Peninsula).
Zhang et al. (2017)	Central-western TP	1979–2013	WAM	ERA-Interim, NCEP-2	More than 21% of the moisture comes from oceans.
Huang et al. (2018)	Southeaster TP	1979–2016 (winter extreme precipitation)	LAGRANTO	ERA-Interim	About 18% of the moisture comes from oceans.
Pan et al. (2018)	Southern/northern TP	1982–2014	CAM	MERRA	During summer, the Indian Ocean supplies about 28.5% of the moisture to the southern TP.
Chen et al. (2019)	Four areas in TP	1980–2016 (May–August)	FLEXPART	ERA-Interim	The northwestern TP and northeastern TP are less affected by the Indian monsoon moisture.
Guo et al. (2019)	TP	1979–2015	WAM-2layers	ERA-Interim	The Indian Ocean and the Pacific Ocean account for 24% and 2% of the moisture contribution, respectively.
Li et al. (2019)	Endorheic TP	1979–2015	WAM-2layers	ERA-Interim, MERRA-2, JRA-55	24%–30% of the moisture comes from oceans.
Qiu et al. (2019)	Three areas in TP	1979–2016 (winter extreme precipitation)	LAGRANTO	ERA-Interim	Moisture contributions of the Arabian Sea to the intense precipitation in the western, south-central, and southeastern TP are 9.2%, 6.9%, and 1.1%, respectively.
Xu and Gao (2019)	Southeaster TP	1982–2011 (April–September)	QIBT	ERA-Interim	Only 2% of the moisture originates from the oceanic source.
Zhang et al. (2019a)	Southern/northern TP	1979–2016	WAM-2layers	ERA-Interim	Northwestern (southeastern) source contributes ~39% (~51%) of the moisture in the northern (southern) TP.
Zhang et al. (2019b)	Sanjiangyuan Region	1960–2017 (June–September)	HYSPLIT, HDBSCAN	NNR1	About 51% (54%) of the medium to heavy precipitation is influenced by the northwestern (southern) source.
Liu et al. (2020)	Western TP	1979–2018 (winter)	HYSPLIT	ERA-Interim	About 57% of the moisture comes from the Arabian Sea, the Arabian Peninsula, and the northern Indian Ocean.

Ma et al. (2020)	Seven areas in TP	1961–2015 (summer extreme event)	HYSPLIT	NCEP/NCAR	About 75% of the moisture for extreme precipitation in the southeastern TP comes from the Bay of Bengal.
Yang et al. (2020)	Southeastern TP	1980–2016 (June–September)	FLEXPART	ERA-Interim	30% of the moisture comes from oceans.
Zhang (2020)	TP	1998–2018	WAM-2layers	ERA-Interim, TRMM	The southeastern source from the TP to the western Indian Ocean accounts for 32% of the moisture contribution.
Li et al. (2022)	Seven basins in TP	1979–2015	WAM-2layers	ERA-Interim, MERRA-2, JRA-55	Oceanic moisture accounts for 24%–30% of the moisture in different basins of the TP.

Table S2: Summary of the selected 17 model layers in three reanalysis products. The column "Pressure" represents the corresponding pressures under standard surface pressure.

	ERA-Interim		MERRA-2		JRA-55	
	Model layer	**Pressure (hPa)**	**Model layer**	**Pressure (hPa)**	**Model layer**	**Pressure (hPa)**
1	60	1012.05	72	1013.25	1	998.50
2	59	1009.06	71	998.05	2	995.50
3	58	1004.64	70	982.77	3	991.50
4	57	998.39	69	967.48	4	985.50
5	56	989.95	68	952.20	5	977.00
6	55	979.06	67	936.91	6	966.00
7	54	965.57	66	921.63	7	953.00
8	51	908.65	65	906.34	9	917.98
9	48	828.05	61	845.21	12	846.96
10	47	796.59	59	809.56	14	786.96
11	44	691.75	55	707.70	17	684.41
12	41	573.38	52	605.88	20	571.90
13	38	461.90	49	491.40	23	458.38
14	35	353.23	46	377.07	26	351.86
15	32	257.36	44	288.93	29	257.36
16	27	132.76	40	150.39	34	132.88
17	17	18.81	28	19.79	44	18.99

Table S3: Relative moisture contribution to the TP precipitation from different western oceans in summer, winter, and on the annual scale.

	The Atlantic	**The Mediterranean**	**The Red Sea**	**The Persian Gulf**
Summer	1.88%	1.05%	0.35%	0.82%
Winter	13.76%	8.43%	5.39%	4.42%
Annual	4.49%	2.75%	1.36%	1.57%

Table S4: The correlation coefficients between monthly precipitation $\delta^{18}O$ and the relative oceanic moisture contribution from the IO for 19 stations (derived from ERA-Interim, MERRA-2, and JRA-55, respectively). '*' represents statistically significant correlation coefficients ($p < 0.05$). To ensure the robustness of correlations, we only calculated the correlation coefficients for stations with available isotope data longer than 10 months.

		Model layers (from the surface to the upper atmosphere)		
		ERA-I	**MERRA-2**	**JRA-55**
Monsoon domain	1.Nyalam	–0.65*	–0.18	–0.51
	2.Zhangmu	-	-	-
	3.Dingri	-	-	-
	4.Larzi	-	-	-
	5.Baidi	–0.37	–0.42	–0.41
	6.Wengguo	-	-	-
	7.Dui	–0.38	–0.49	–0.33
	8.Lhasa	–0.62*	–0.44	–0.52
	9.Yangcun	-	-	-
	10.Nagqu	–0.39	–0.18	–0.05
	11.Lulang	–0.44	–0.12	–0.29
	12.Nuxia	-	-	-
	13.Bomi	–0.05	0.30	0.16
Transition domain	14.Shiquanhe	-	-	-
	15.Gaize	–0.73*	–0.52*	–0.36
	16.Tuotuohe	–0.80*	–0.63*	–0.36
	17.Yushu	–0.06*	0.04	0.32
Westerlies domain	18.Taxkorgen	–0.87*	–0.87*	–0.84*
	19.Delingha	–0.84*	–0.84*	–0.75*

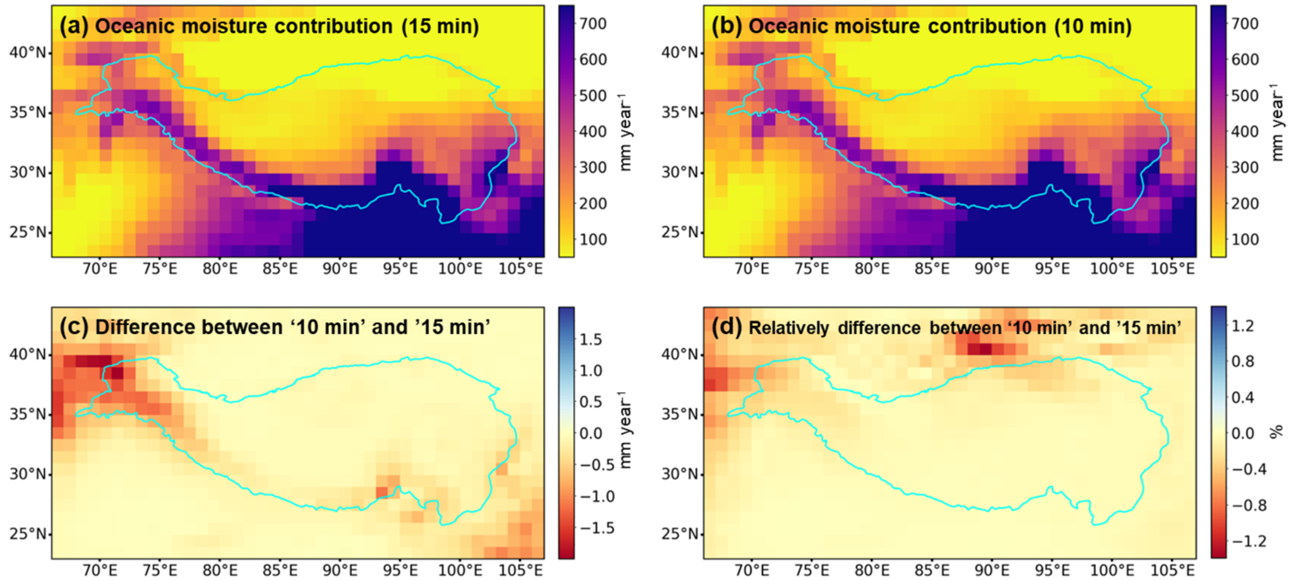

Figure S1: Mean annual oceanic moisture contribution to the TP precipitation simulated using (a) 15 min (0.25 h) time step and (b) 10 min time step, and (c) the absolute difference and (d) the relative difference (%) between these two simulations. The forcing dataset is ERA-Interim. Cyan lines represent the TP boundary.

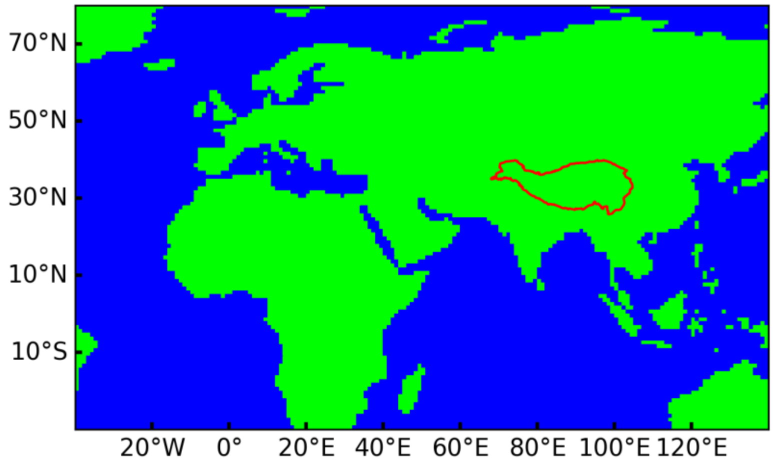

Figure S2: The land-sea mask used in this study with 1°×1° spatial resolution (the blue area represents oceans). Red line represents the TP boundary.

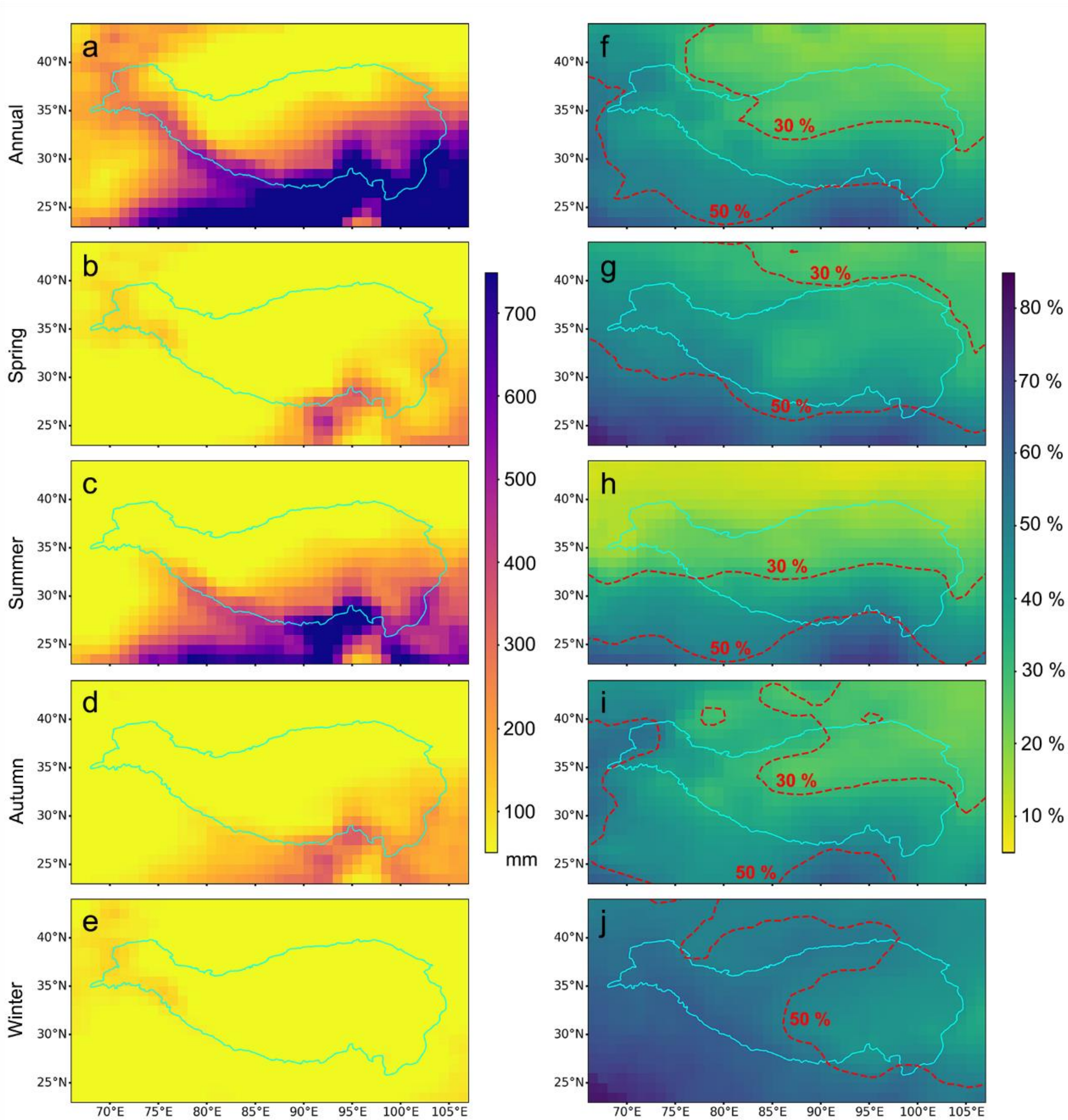

Figure S3: Same as Figure 1 but based on MERRA-2 (1980–2015).

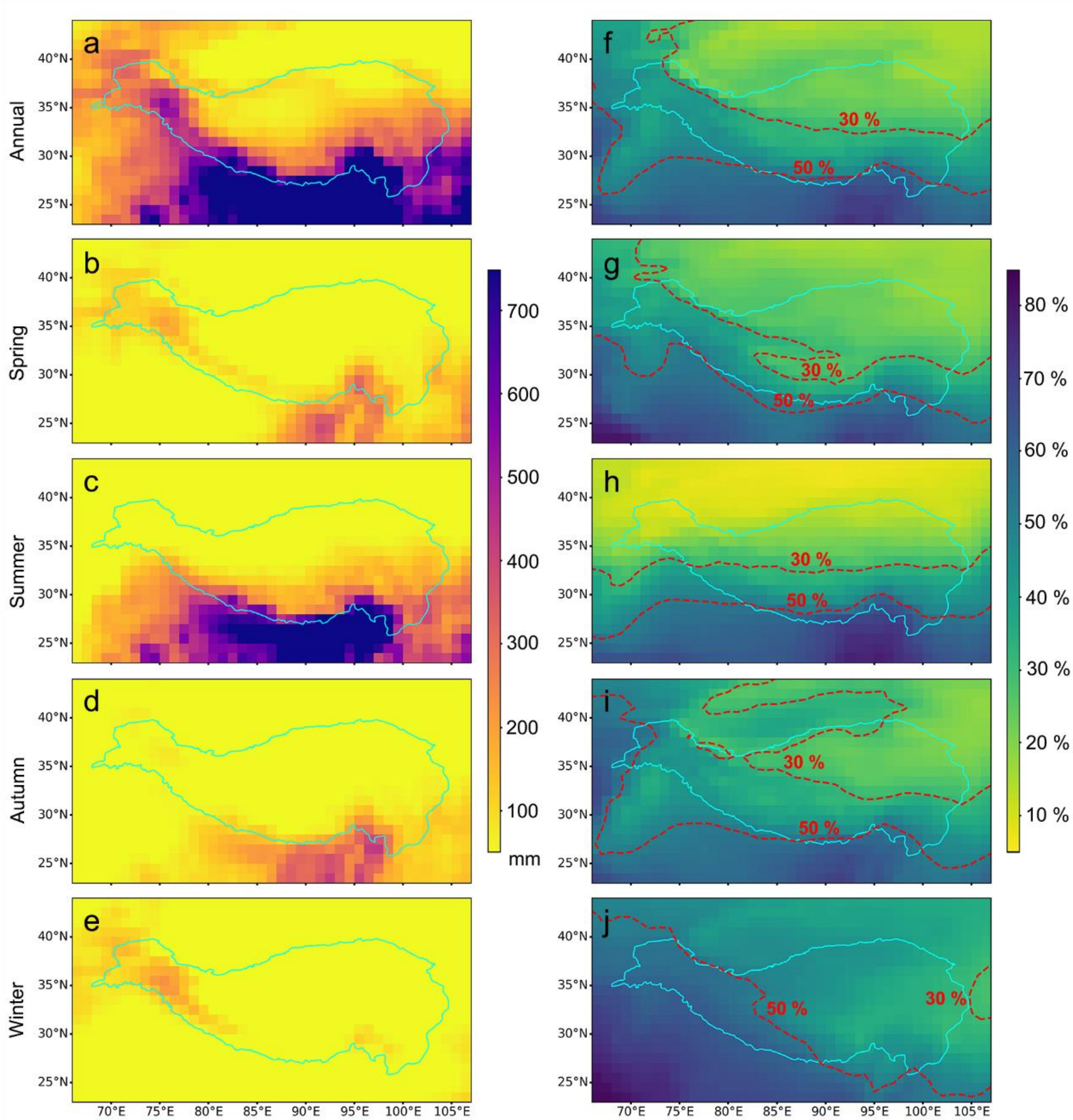

Figure S4: Same as Figure 1 but based on JRA-55 (1979–2015).

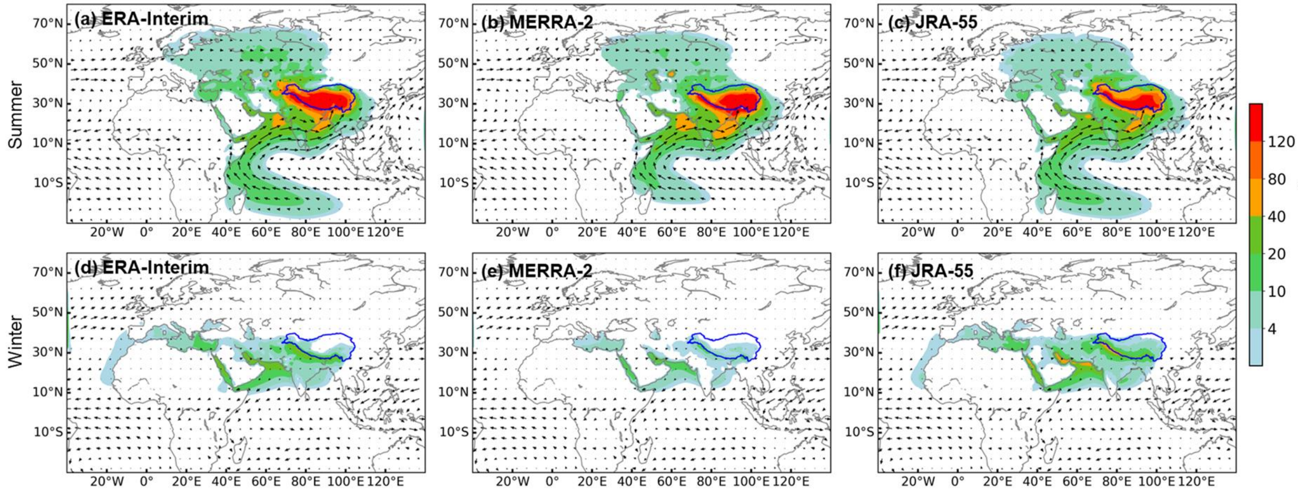

Figure S5: Mean moisture sources of the TP precipitation in (a–c) summer and (d–f) winter. Blue lines represent the location of the TP. Moisture sources (shown as equivalent water height) are tracked backward using the WAM-2layers driven by three forcing datasets (ERA-Interim, MERRA-2, and JRA-55).

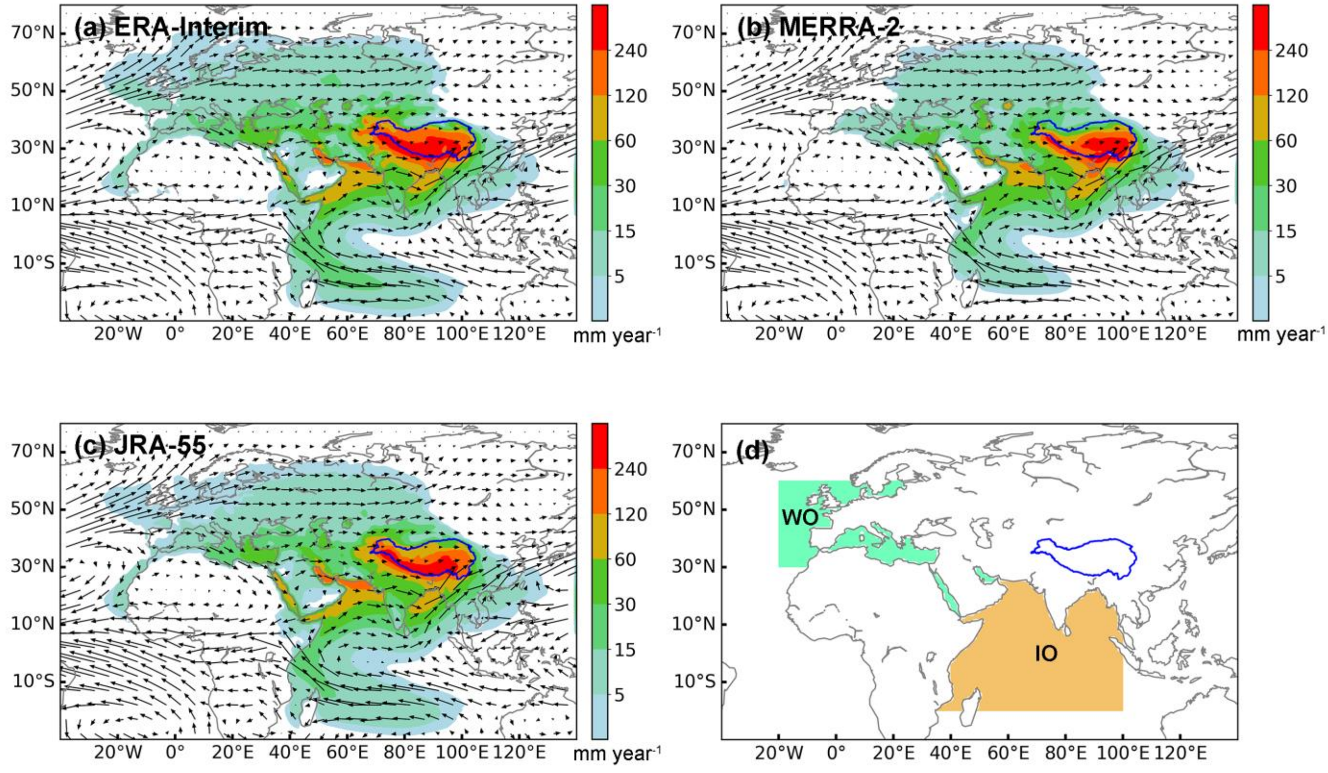

Figure S6: (a–c) Mean annual moisture sources of the TP precipitation and (d) the partition of the western oceans (WO) and the Indian Ocean (IO). Blue lines represent the location of the TP. Moisture sources are tracked backward using the WAM-2layers driven by three forcing datasets (ERA-Interim, Merra-2, and JRA-55).

45

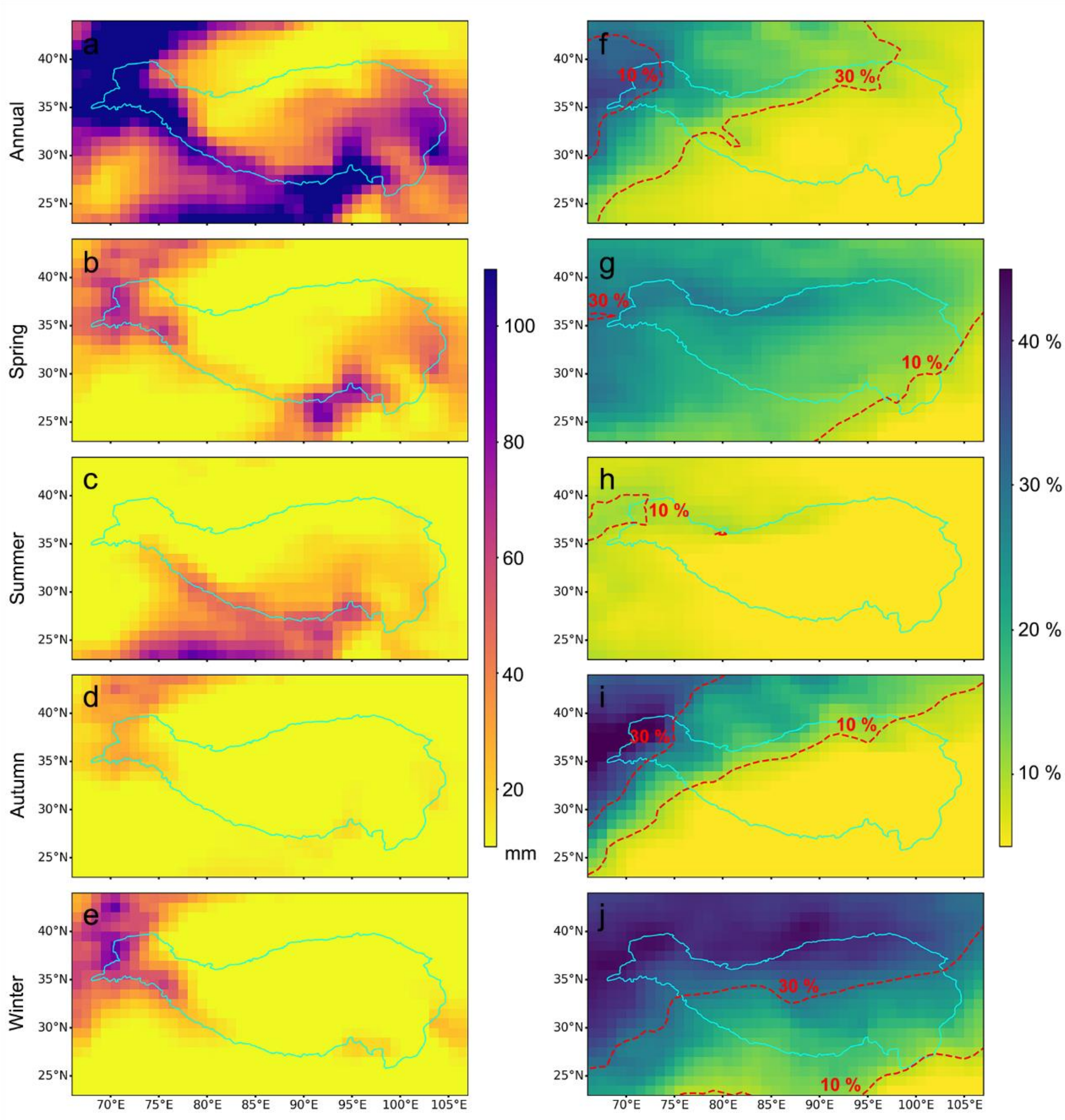

Figure S7: Same as Figure 3 but based on MERRA-2 (1980–2015).

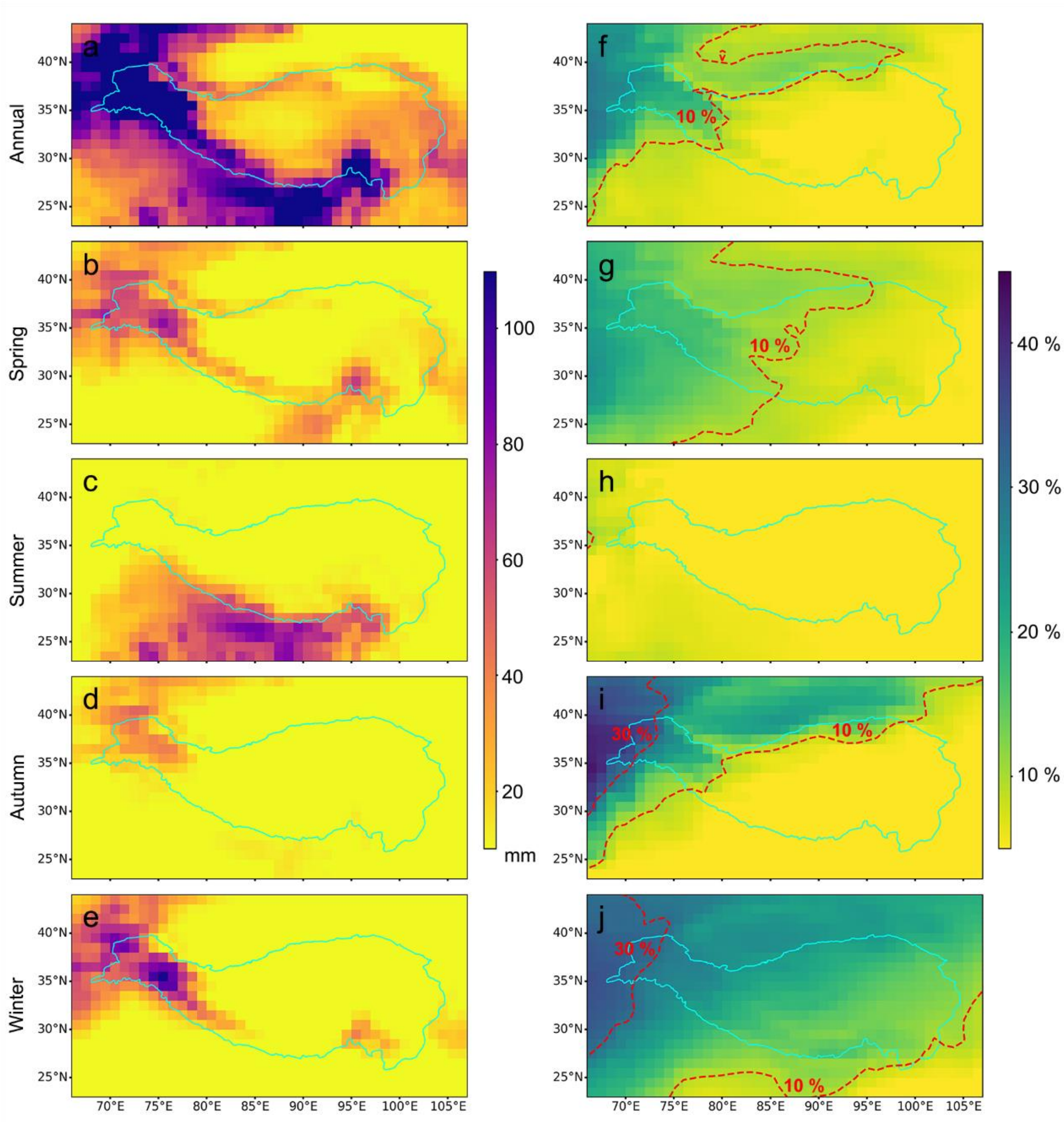

Figure S8: Same as Figure3 but based on JRA-55 (1979–2015).

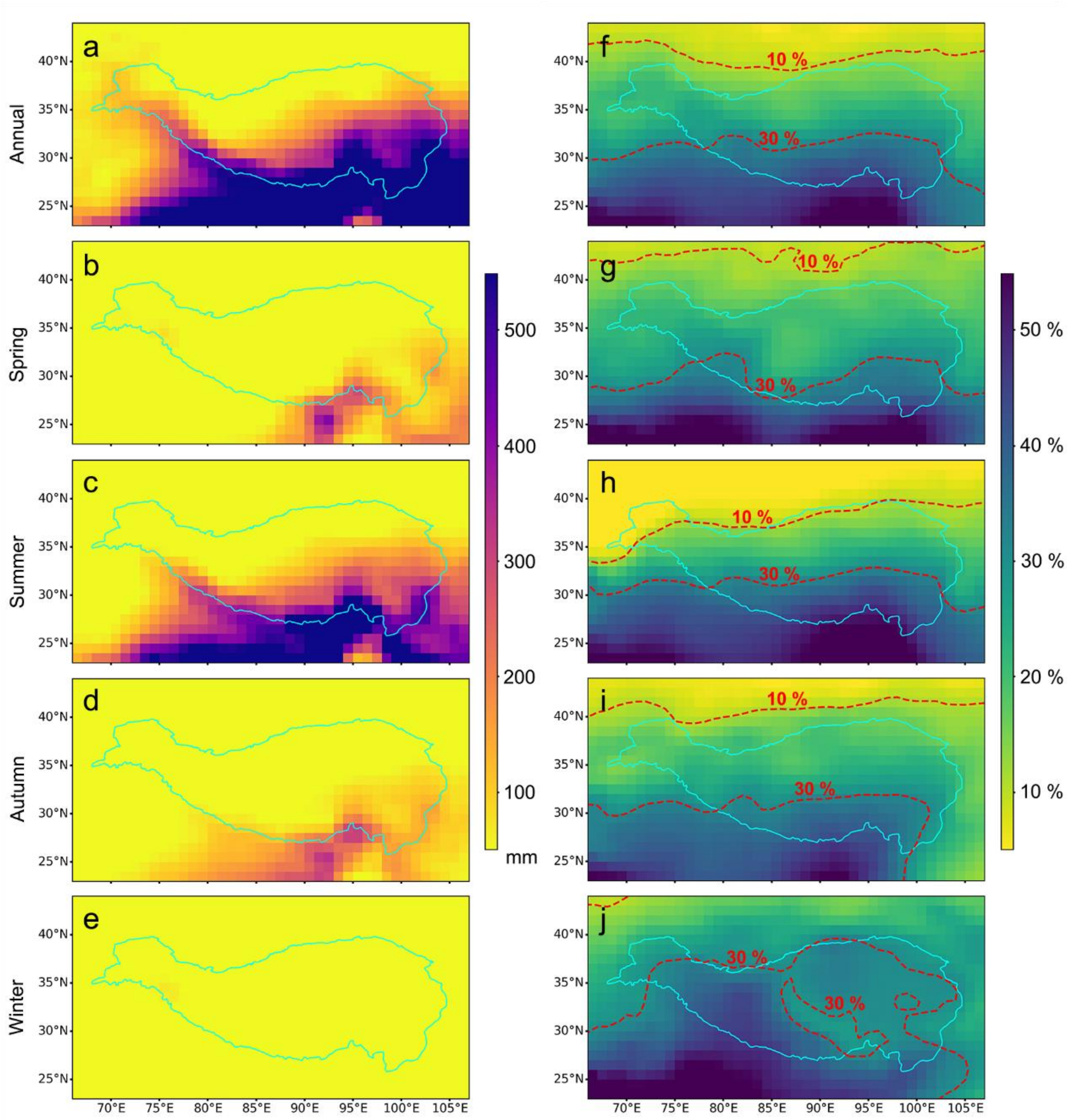

Figure S9: Same as Figure 4 but based on MERRA-2 (1980–2015).

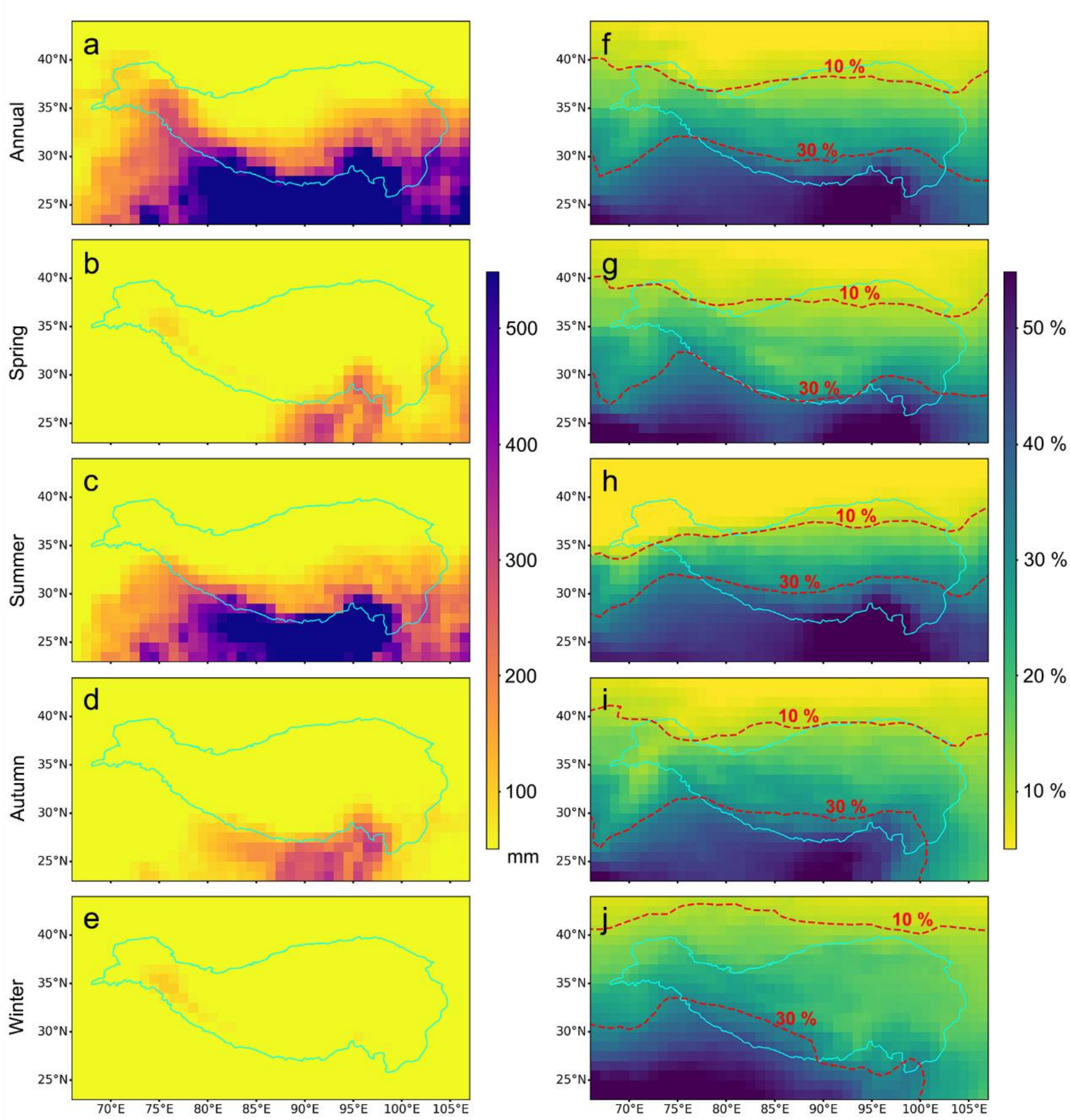

55 **Figure S10:** Same as Figure 4 but based on JRA-55 (1979–2015).

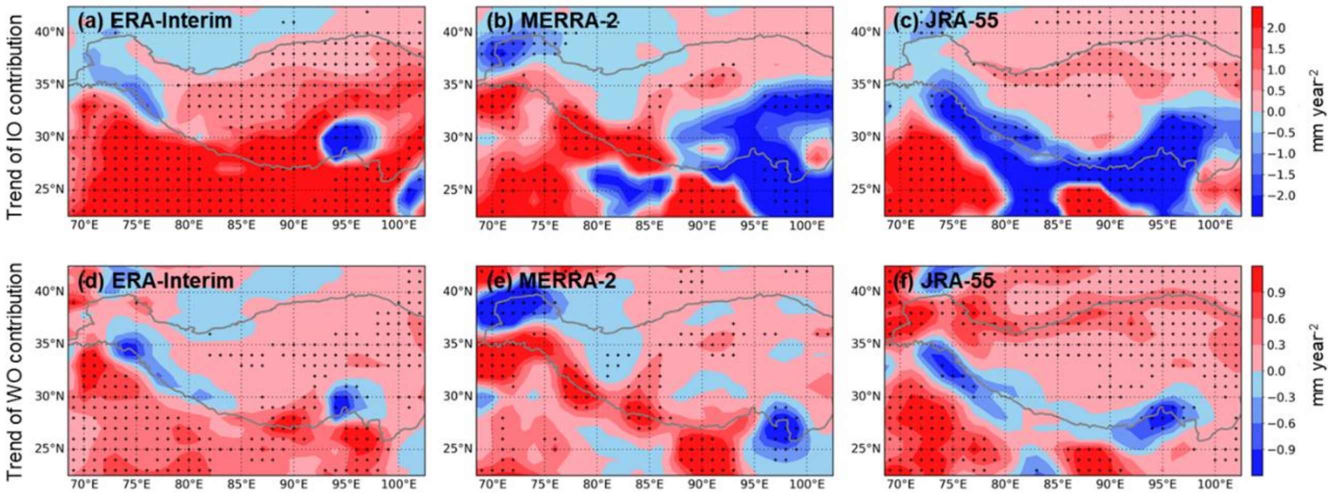

Figure S11: Trends of oceanic moisture contribution to the TP precipitation from (a–c) the Indian Ocean (IO) and (d–f) the western oceans (WO), on the annual scale using ERA-Interim (1979–2015), MERRA-2 (1980–2015), and JRA-55 (1979–2015). Stippling indicates regions with statistically significant trends ($p < 0.05$).

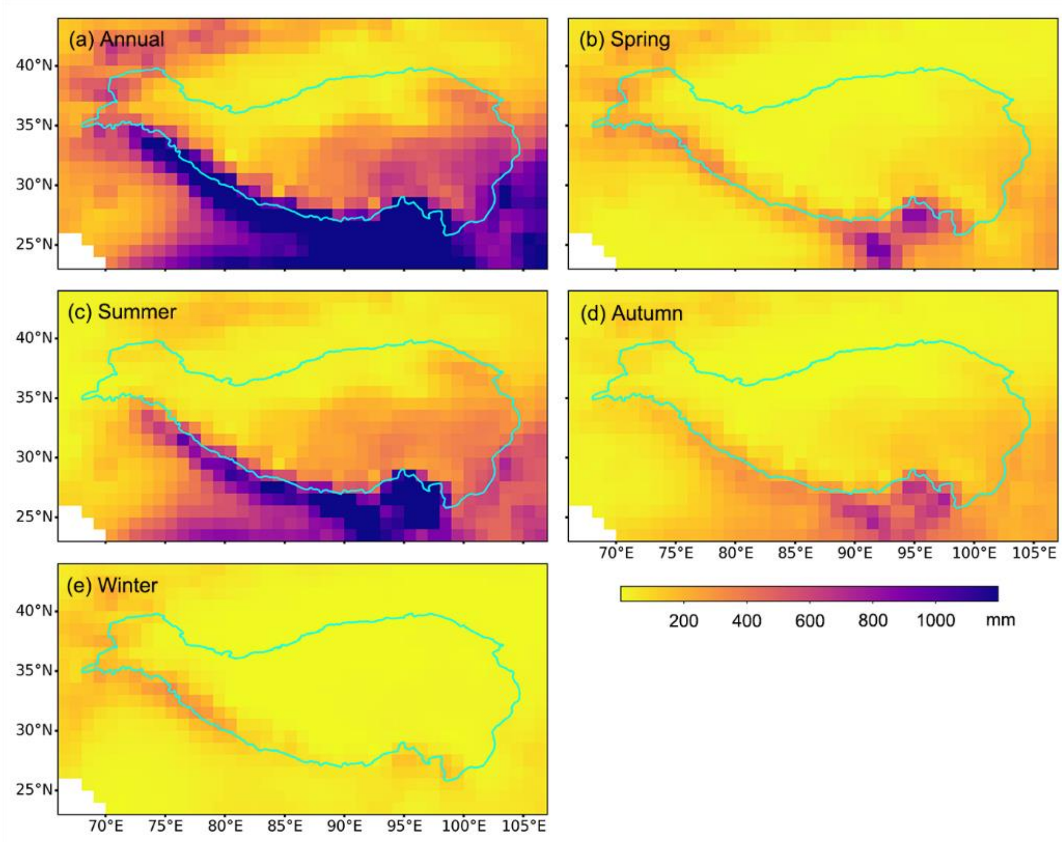

Figure S12: Long-term mean precipitation distributions over the TP on annual and seasonal scales based on Global Precipitation Climatology Centre (GPCC) Full Data Monthly Version precipitation (*Schneider et al.*, 2018) during 1979–2015.

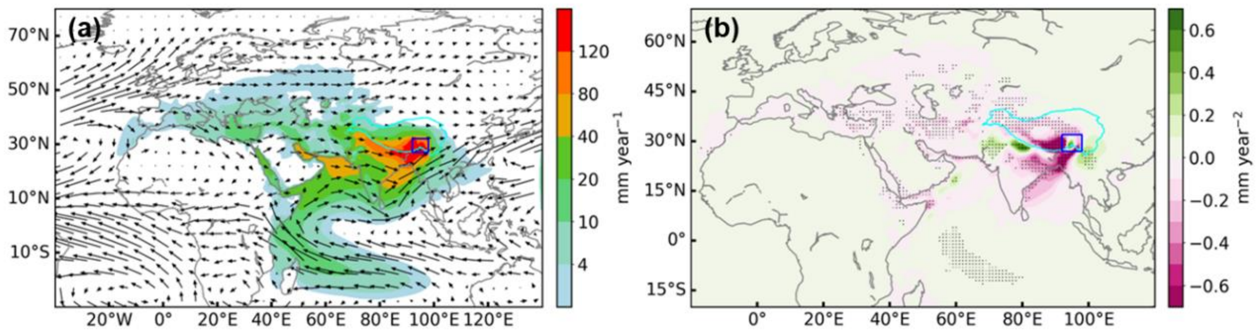

Figure S13: (a) Long-term mean annual moisture source to precipitation in the SETP and (b) the relevant trends of moisture contributions during 1979–2015 simulated by using WAM-2layers driven by ERA-Interim. The blue rectangles represent the SETP. Stippling in (b) indicates regions with statistically significant trends ($p < 0.05$).

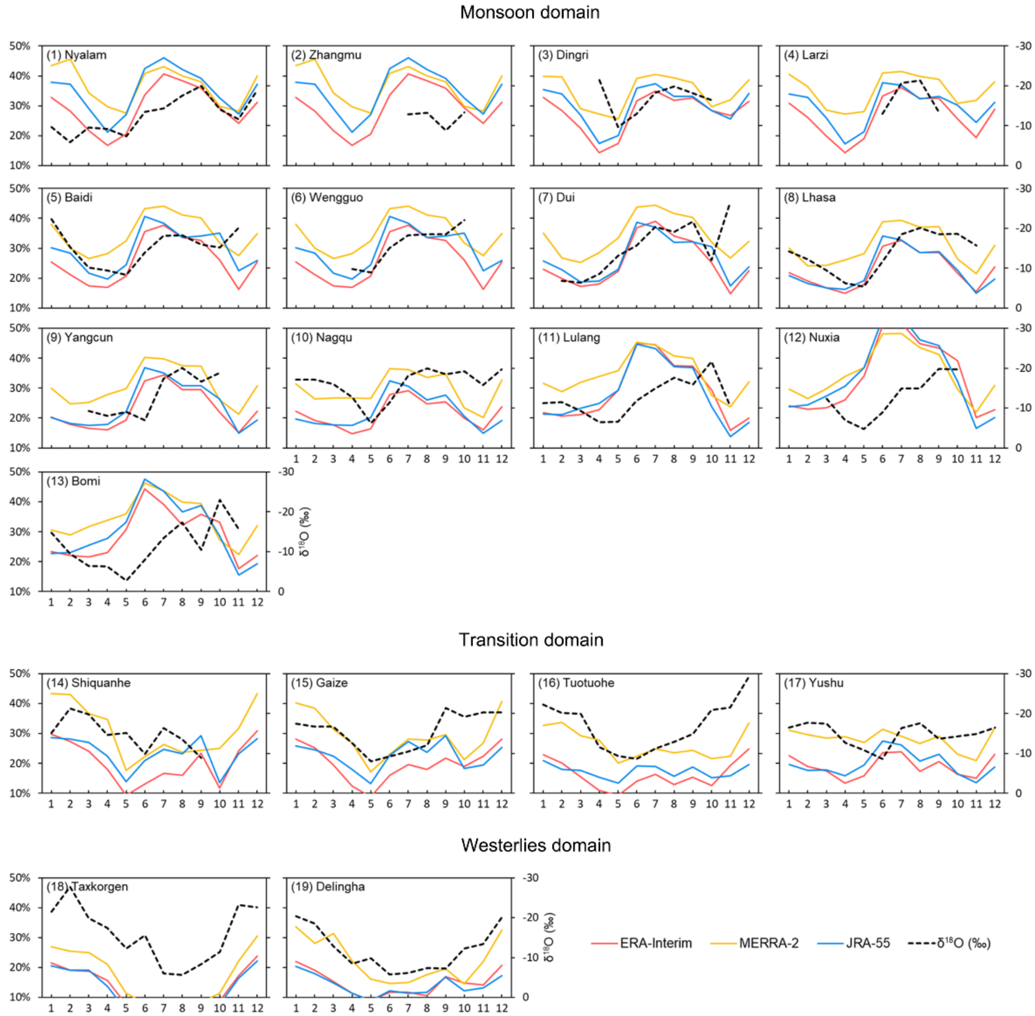

Figure S14: The relationship between monthly relative contributions of moisture from IO in three simulations and precipitation isotope observations at 19 stations.

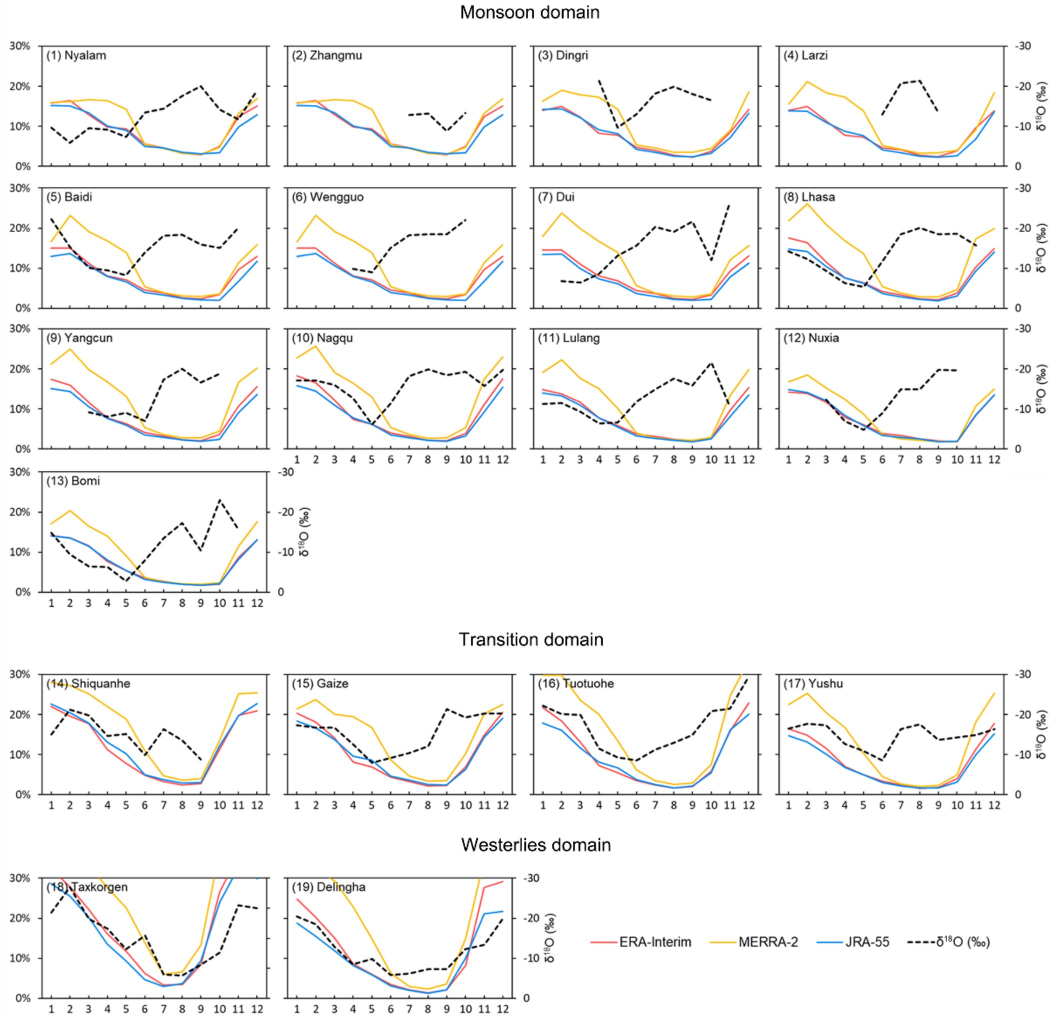

Figure S15: Same as Figure S14 but for relative moisture contribution from WO.

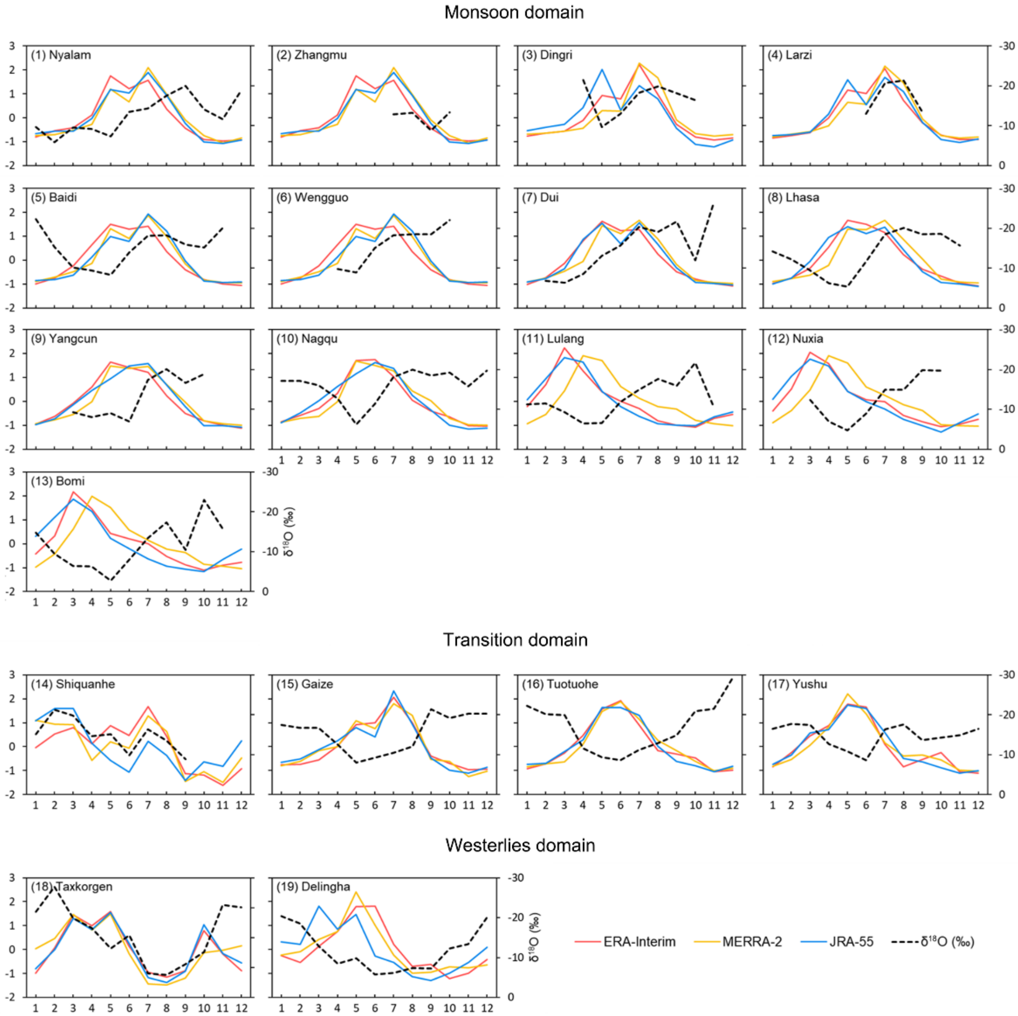

Figure S16: Same as Figure S14 but for absolute moisture contribution from WO. All absolute contributions are standardized with Z-scores method.

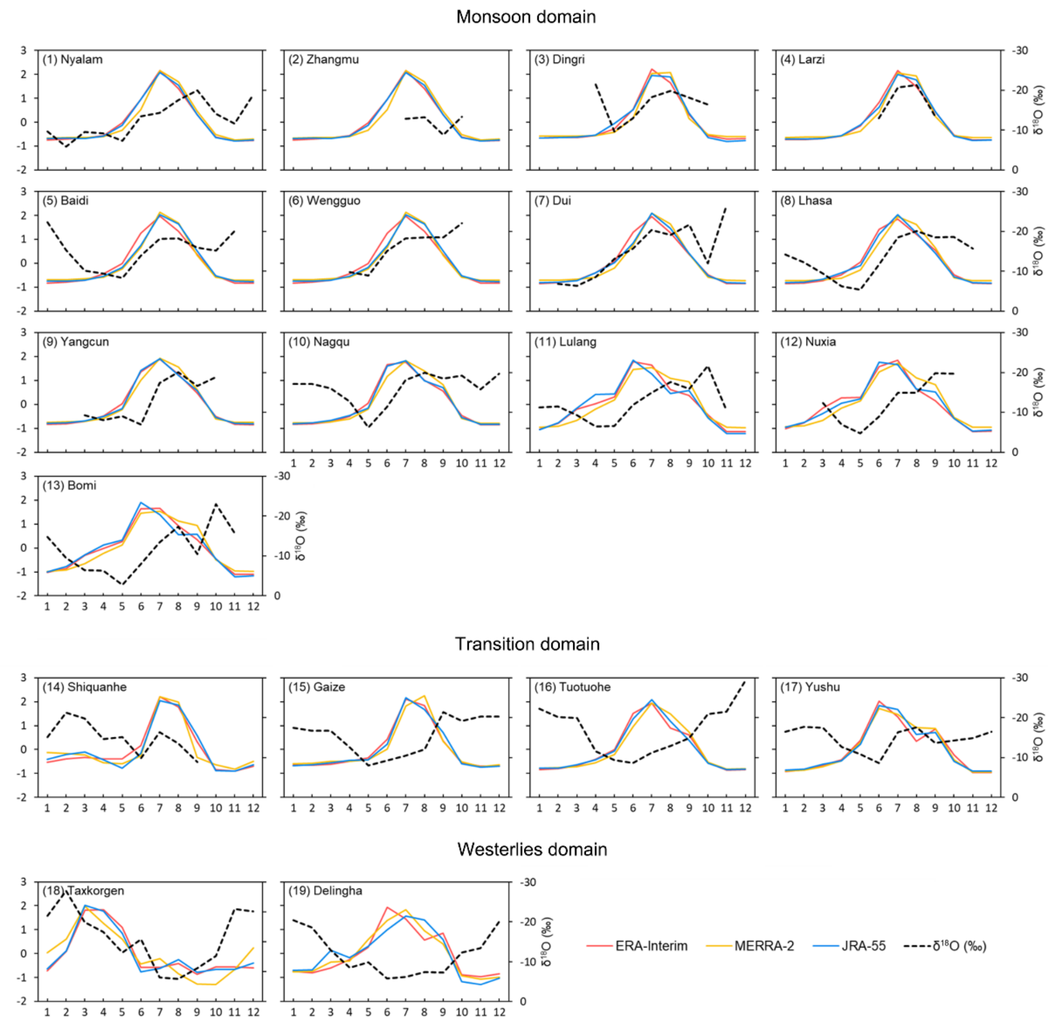

Figure S17: Same as Figure S14 but for absolute moisture contribution from IO. All absolute contributions are standardized with Z-scores method.

85

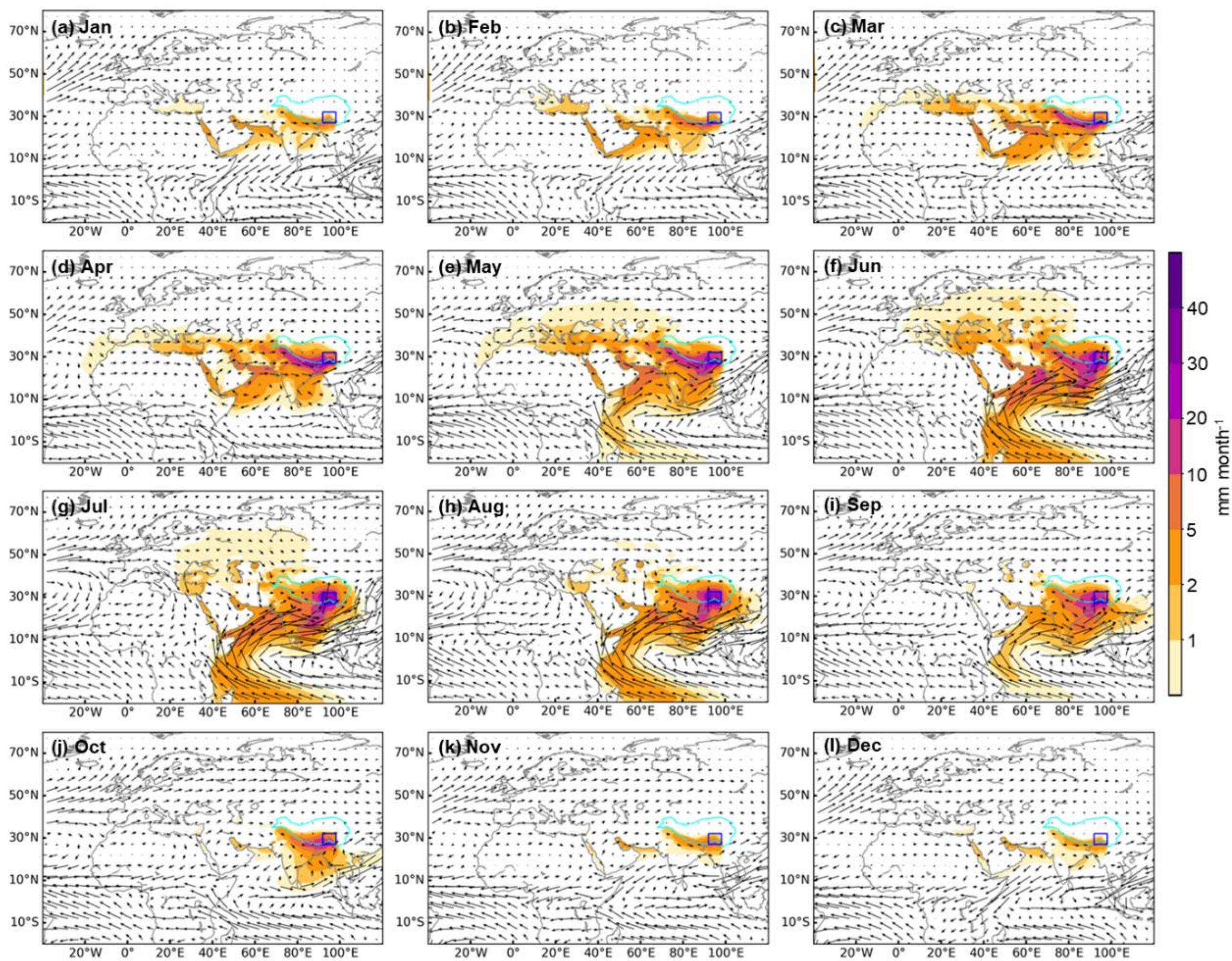

Figure S18. Mean monthly moisture sources of precipitation in the SETP simulated using WAM-2layers driven by ERA-Interim (1979–2015). The blue rectangle represents the SETP.

References:

Chen, B., Xu, X. D., Yang, S., and Zhang, W.: On the origin and destination of atmospheric moisture and air mass over the Tibetan Plateau, Theor. Appl. Climatol., 110(3), 423-435, https://doi.org/10.1007/s00704-012-0641-y 2012.

Chen, B., Zhang, W., Yang, S., and Xu, X. D.: Identifying and contrasting the sources of the water vapor reaching the subregions of the Tibetan Plateau during the wet season, Climate Dyn., 53(11), 6891-6907, https://doi.org/10.1007/s00382-019-04963-2, 2019.

Guo, L., van der Ent, R. J., Klingaman, N. P., Demory, M.-E., Vidale, P. L., Turner, A. G., Stephan, C. C., and Chevuturi, A.: Moisture Sources for East Asian Precipitation: Mean Seasonal Cycle and Interannual Variability, J. Hydrometeorol., 20(4), 657-672, https://doi.org/10.1175/jhm-d-18-0188.1, 2019.

Huang, W., Qiu, T., Yang, Z., Lin, D., Wright, J. S., Wang, B., and He, X.: On the formation mechanism for wintertime extreme precipitation events over the southeastern Tibetan Plateau, J. Geophys. Res.-Atmos., 123(22), 12,692-612,714, https://doi.org/10.1029/2018JD028921 2018.

Li, Y., Su, F., Chen, D., and Tang, Q.: Atmospheric Water Transport to the Endorheic Tibetan Plateau and Its Effect on the Hydrological Status in the Region, J. Geophys. Res.-Atmos., 124(23), 12864-12881, https://doi.org/10.1029/2019jd031297, 2019.

Li, Y., Su, F., Tang, Q., Gao, H., Yan, D., Peng, H., and Xiao, S.: Contributions of moisture sources to precipitation in the major drainage basins in the Tibetan Plateau, Sci. China-Earth Sci., 65(1674-7313), 1088, https://doi.org/https://doi.org/10.1007/s11430-021-9890-6, 2022.

Liu, X., Liu, Y., Wang, X., and Wu, G.: Large-Scale Dynamics and Moisture Sources of the Precipitation Over the Western Tibetan Plateau in Boreal Winter, J. Geophys. Res.-Atmos., 125(9), e2019JD032133, https://doi.org/10.1029/2019JD032133, 2020.

Ma, Y., Lu, M., Bracken, C., and Chen, H.: Spatially coherent clusters of summer precipitation extremes in the Tibetan Plateau: Where is the moisture from?, Atmos. Res., 237, 104841, https://doi.org/10.1016/j.atmosres.2020.104841, 2020.

Pan, C., Zhu, B., Gao, J., Kang, H., and Zhu, T.: Quantitative identification of moisture sources over the Tibetan Plateau and the relationship between thermal forcing and moisture transport, Climate Dyn., 52(1-2), 181-196, https://doi.org/10.1007/s00382-018-4130-6, 2018.

Qiu, T., Huang, W., Wright, J. S., Lin, Y., Lu, P., He, X., Yang, Z., Dong, W., Lu, H., and Wang, B.: Moisture Sources for Wintertime Intense Precipitation Events Over the Three Snowy Subregions of the Tibetan Plateau, J. Geophys. Res.-Atmos., 124(23), 12708-12725, https://doi.org/10.1029/2019jd031110, 2019.

Schneider, U., Becker, A., Finger, P., Meyer-Christoffer, A., and Ziese, M.: GPCC Full Data Monthly Product Version 2018 at 1.0°: Monthly Land-Surface Precipitation from Rain-Gauges built on GTS-based and Historical Data, Global Precipitation Climatology Centre (GPCC), https://doi.org/10.5676/DWD_GPCC/FD_M_V2018_100, 2018.

Sun, B., and Wang, H.: Moisture sources of semiarid grassland in China using the Lagrangian particle model FLEXPART, J. Climate, 27(6), 2457-2474, https://doi.org/10.1175/JCLI-D-13-00517.1 2014.

Xu, Y., and Gao, Y.: Quantification of Evaporative Sources of Precipitation and Its Changes in the Southeastern Tibetan Plateau and Middle Yangtze River Basin, Atmosphere, 10(8), 428, https://doi.org/10.3390/atmos10080428, 2019.

Yang, S., Zhang, W., Chen, B., Xu, X., and Zhao, R.: Remote moisture sources for 6-hour summer precipitation over the Southeastern Tibetan Plateau and its effects on precipitation intensity, Atmos. Res., 236, 104803, https://doi.org/10.1016/j.atmosres.2019.104803, 2020.

Zhang, C.: Moisture source assessment and the varying characteristics for the Tibetan Plateau precipitation using TRMM, Environ. Res. Lett., 15(10), 104003, https://doi.org/10.1088/1748-9326/abac78, 2020.

Zhang, C., Tang, Q., and Chen, D.: Recent changes in the moisture source of precipitation over the Tibetan Plateau, J. Climate, 30(5), 1807-1819, https://doi.org/10.1175/JCLI-D-15-0842.1, 2017.

Zhang, C., Tang, Q. H., Chen, D. L., van der Ent, R. J., Liu, X. C., Li, W. H., and Haile, G. G.: Moisture Source Changes Contributed to Different Precipitation Changes over the Northern and Southern Tibetan Plateau, J. Hydrometeorol., 20(2), 217-229, https://doi.org/10.1175/Jhm-D-18-0094.1, 2019a.

Zhang, Y., Huang, W., and Zhong, D.: Major Moisture Pathways and Their Importance to Rainy Season Precipitation over the Sanjiangyuan Region of the Tibetan Plateau, J. Climate, 32(20), 6837-6857, https://doi.org/10.1175/jcli-d-19-0196.1, 2019b.